Influence of Spatially Variable Side Friction and Collocated Data on Single and Multiple Shaft Resistances

Harald Klammler[1]; Michael McVay[2]; Peter Lai[3]; and David Horhota[4]

Abstract: Reliability-based design, such as LRFD, aims at meeting desired probability of failure levels for engineered structures. The present work attempts to contribute to this field by analyzing the influence of spatially variable soil/rock strength on the axial resistance uncertainty of single and multiple shafts in group layouts. This includes spatial variability over the individual shaft surfaces, effects of limited data, random measurement errors, and workmanship. A possible correlation between boring data inside or near the footprint of a foundation and the foundation itself is considered. In a geostatistical approach, spatial averaging (upscaling) and a degenerate case of ordinary kriging are applied to develop variance reduction charts and design equations for a series of foundation group layouts (single, double, triple, and quadruple). For the potential situation of an unknown horizontal correlation range at a site, the worst case scenarios are identified and demonstrated in an example problem. Resulting probabilities of failure are applied to the whole foundation (i.e., group) rather than single objects. It is found that a boring at the center of a group footprint can significantly reduce resistance prediction uncertainty, especially under the worst case scenario for unknown horizontal correlation range. In contrast, independent of the presence of a center boring or not, the uncertainty reduction through additional borings becomes small, once four or five borings are available. **DOI:** 10.1061/(ASCE)GT.1943-5606.0000728.

CE Database subject headings: Load and resistance factor design; Shear resistance; Spatial analysis; Deep foundations; Shafts; Data analysis.

Author keywords: LRFD; Shear resistance; Spatial analysis; Deep foundations.

Introduction

The need and advantages of reliability-based foundation design, such as LRFD, have been widely recognized in existing research and standardization literature (AASHTO 2004; Phoon et al. 2003). The fundamental idea is to use a probabilistic design framework, which rationally accounts for inherent uncertainties in both the load and resistance parameters, to not exceed a prescribed target probability of failure independent of site/job-specific characteristics. Given a particular design-load distribution (e.g., mean/nominal load, coefficient of variation, and lognormality) as a function of superstructure properties, the geotechnical engineer has to estimate a foundation's probabilistic resistance distribution. With load and resistance distributions in hand, the probability of failure may be computed and the foundation design adjusted to meet a target value. In the case of existing foundations, this process may occur in the inverse direction in that a respective resistance distribution is evaluated first, for which a maximum admissible load (distribution) is then defined. For practical design in the LRFD context, foundation resistance uncertainty is accounted for by multiplication of a nominal resistance value with a so-called resistance factor, which is typically smaller than one.

A considerable amount of work has been dedicated to evaluating and processing the different sources of uncertainty involved. Limiting attention to the resistance side, these sources may be categorized into four principal classes: (1) spatial variability of ground properties, (2) measurement errors, (3) uncertainty in data transformation, and (4) construction workmanship (Phoon and Kulhawy 1999a, b). A method to estimate a lump value of all uncertainty types is based on past experience and the compilation and analysis of comprehensive load test databases, which allow for assessment of prediction error distributions (and possibly model calibration) for different combinations of site conditions, prediction, and construction methods (Haldar and Sivakumar Babu 2008; Zhang et al. 2008; Zhang et al. 2001). However, inherent shortcomings with this method are that it does not offer an explicit possibility to account for site specific data, and the characteristics of a site/job have to be matched with a sufficient number of corresponding observations from the past. As an alternative, general approaches have been proposed that evaluate the contributing sources of uncertainty separately and then combine them according to appropriate physical and statistical laws (Foye et al. 2006; Phoon and Kulhawy 1999a, b). Approaches that explicitly account for spatial variability are not very abundant; however, there are several studies considering shallow foundations in two (Sivakumar Babu et al. 2006; Popescu et al. 2005; Fenton and Griffiths 2002, 2003; Paice et al. 1996) and three (Fenton and Griffiths 2005) dimensions. Fenton et al. (2005, 2008) relate their previous results to the LRFD context and investigate effects of data in the vicinity of a shallow foundation to reduce resistance

[1]Research Fellow, Dept. of Environmental Science and Sustainable Development, Federal Univ. of Bahia, Rua Professor Jose Seabra s/n, Barreiras, 47805 Bahia, Brazil (corresponding author). E-mail: haki@gmx.at

[2]Professor, Dept. of Civil and Coastal Engineering, Univ. of Florida, 365 Weil Hall, Gainesville, FL 32611. E-mail: mcm@ce.ufl.edu

[3]Assistant State Geotechnical Engineer, Florida Dept. of Transportation, 605 Suwannee St., Tallahassee, FL 32399. E-mail: peter.lai@dot.state.fl.us

[4]State Geotechnical Material Systems Engineer, Florida Dept. of Transportation, State Materials Office, 5007 Northeast 39th Ave., Gainesville, FL 32609. E-mail: david.horhota@dot.state.fl.us

Note. This manuscript was submitted on November 18, 2010; approved on March 12, 2012; published online on March 14, 2012. Discussion period open until June 1, 2013; separate discussions must be submitted for individual papers. This paper is part of the ***Journal of Geotechnical and Geoenvironmental Engineering***, Vol. 139, No. 1, January 1, 2013. ©ASCE, ISSN 1090-0241/2013/1-84–94/$25.00.

uncertainty. Furthermore, Fenton and Griffiths (unpublished report, 2007) present a preliminary study for a single object deep foundation subject to vertically variable ground properties. In contrast, reliabilities of deep foundations in the form of pile groups are evaluated by Zhang et al. (2001) based on a respective load test database, however, without explicit consideration of spatial variability or nearby data.

Based on a geostatistical approach, Klammler et al. (2010a) investigate the influence of spatially variable side friction on the ultimate resistance and LRFD resistance factors of single drilled shafts against axial loads. The present work expands on this work by considering (1) multiple shaft foundations under rigid pile caps (which are assumed to not contribute to the foundation resistance), (2) conditioning data inside or near a foundation's footprint (single or group layouts), and (3) random measurement and construction uncertainties. According to current practice in Florida limestone (Florida Department of Transportation [FDOT] 2011), resistance contributions of end bearing are hereby neglected. For this purpose, a (geo)statistical approach (Isaaks and Srivastava 1989; Journel and Huijbregts 1978) is adopted with the following notation: $q(x)$ (stress)—or in short q—denotes a spatially variable (random) function for local side friction (i.e., strength or cohesion at zero confining pressure) with x (length) being a spatial coordinate vector. For instance, in the case of rock, the measured local values of q at a site may be available from core sampling and laboratory testing using $q = \rho(q_u q_t)^{1/2}/2$, where q_u (stress) is the unconfined compression strength, q_t (stress) is the split tension strength, and ρ (dimensionless) is the local recovery (FDOT 2011; Chung et al. 2011). Similarly, for soil, the cone penetrometer (CPT) tip resistance at a given depth multiplied by a soil and installation method factor may be used to assess local side friction q (Brustamante and Gianeselli 1982). Regardless of the method, q is described by a mean μ_q (stress), variance σ_q^2 (stress^2), and a spatial covariance function $C_q(h)$—or in short C_q (stress^2)—with h (length) being a spatial separation vector between two locations x_1 and x_2. C_q may be anisotropic with a correlation range a_h (length) in all horizontal directions and a correlation range a_v (length) in the vertical direction. A normalized spatial covariance function $C'_q(h_{\text{iso}}) = C_q(h_{\text{iso}})/\sigma_q^2$ of unit sill and unit isotropic range may be defined using $h_{iso} = \sqrt{(h_h/a_h)^2 + (h_v/a_v)^2}$, where h_h and h_v (both length) are the horizontal and vertical separation vector components, respectively, between two locations. f_s (stress) with mean μ_s (stress) and variance σ_s^2 (stress^2) is a random function used to describe the mean unit side friction over the lateral surface of area A_s (area) of a single shaft of diameter D (length) and embedment length L (length). Similarly, f_f with mean μ_f (stress) and variance σ_f^2 (stress^2) is a random function used to represent the mean unit side friction over the lateral surface of area A_f of all n_s (dimensionless) shafts of diameter D, length L, and fundamental center-to-center separation distance D_s (length) in the group foundation. Finally, R_n (force) and CV_R (dimensionless) denote the foundation nominal resistance (defined as the mean of the random foundation resistance R [force]) as a result of side friction at the ultimate limit state and the respective coefficient of variation as a measure of uncertainty, which are used in determining the LRFD resistance factor Φ (dimensionless).

Theoretical Development

Multiple Shaft Foundations without Nearby Data

As opposed to single shaft foundations, failure of multiple shaft foundations in a group from axial loads may occur in one of two different forms: (1) along the set of disjoint lateral surfaces encompassing all of the individual shafts or (2) along a single surface enclosing all shafts of a foundation or group (block failure). For $D_s/D > 2$, block failure may not be expected to occur (Zhang et al. 2001), and Scenario 1 will be investigated with results presented for a typical value of $D_s/D = 3$. As in Klammler et al. (2010a), it is assumed that the geostatistical parameters of q (i.e., μ_q, σ_q^2, and C_q) within a geostatistically homogeneous site (or subzone thereof), are well known, which may be the case because of exhaustive rock core sampling or CPT soil testing, for example. If end bearing is neglected (FDOT 2011), Eq. (1) describes the simple relationship between f_f and total foundation resistance R as

$$R = A_f f_f \tag{1}$$

where $A_f = n_s L D \pi$ is considered deterministic, that is, with negligible uncertainty compared with f_f, and n_s is the number of shafts in a foundation. Based on a study of a series of load tests (FDOT 2003), Eq. (1) assumes that local side friction at the ultimate limit state is fully mobilized and, hence, deformation independent. R and f_f are random variables linked to q by the spatial upscaling (arithmetic averaging) process

$$f_f = \frac{1}{A_f} \int_{A_f} q \times dA \tag{2}$$

By taking the expectation and variance of Eq. (2), the parameters μ_f and σ_f^2 are found as (Journel and Huijbregts 1978)

$$\mu_f = \mu_q \tag{3}$$

$$\sigma_f^2 = \frac{\sigma_q^2}{A_f^2} \int_{A_f} \int_{A_f} C'_q dA_1 dA_2 \tag{4}$$

where a variance reduction factor α_{qf} (dimensionless) between local strength q and mean foundation unit side friction f_f may be defined as

$$\alpha_{qf} = \frac{\sigma_f^2}{\sigma_q^2} = \alpha_{sf} \frac{\sigma_s^2}{\sigma_q^2} = \alpha_{sf} \alpha_{qs} \tag{5}$$

which links the variability in local strength q to the uncertainty in foundation or group resistance R by $\text{CV}_R = \alpha_{qf}^{1/2} \text{CV}_q$ (where CV is the notation for the coefficient of variation of the variable in the index). α_{sf} in Eq. (5) denotes an intermediate variance reduction factor between single shaft unit side friction f_s and the foundation unit side friction f_f. Furthermore, α_{qs} quantifies the variance reduction between local strength q and f_s, as studied by Klammler et al. (2010a). The double integral in Eq. (4) is nothing but the summation of the normalized covariance values between all possible combinations of point pairs on the n_s lateral shaft surfaces (i.e., the sum of all elements in the variance-covariance matrix between all possible point pairs) and may be evaluated numerically by discretizing each shaft surface into a large enough number of points (Journel and Huijbregts 1978). Calculations may hereby be accelerated by recognizing that center-to-center separation distances between different shaft pairs are limited to a certain pattern (e.g., $3D$ for all shaft pairs on a side of a quadruple square foundation and $3\sqrt{2}D$ for shaft pairs on a diagonal). Thus, normalized covariances $C'_q(h_s) = C_s(h_s)/\sigma_s^2$ (dimensionless) between upscaled single shaft resistances f_s (with h_s [length] representing the horizontal separation distance between shaft centers) may be determined for these separation distances using Eq. (6) (Journel and Huijbregts 1978) to populate a respective

J. Geotech. Geoenviron. Eng. 2013.139:84-94.

variance-covariance matrix between all individual shafts in a foundation through

$$C'_q(h_s) = \frac{\sigma_q^2}{\sigma_s^2 A_{s1} A_{s2}} \int_{A_{s1}} \int_{A_{s2}} C'_q dA_1 dA_2 \tag{6}$$

where A_{s1} and A_{s2} = lateral surface areas of two horizontally offset shafts. Eq. (6) is, in fact, a generalization of Eq. (4) (normalized to σ_s^2, i.e., unit sill), which is obtained by setting $A_{s1} = A_{s2} = A_f$, that is, the total of all shaft's lateral surfaces. For $A_{s1} = A_{s2} = LD\pi$, that is, a single shaft's lateral surface or zero separation between two shafts, Eq. (6) reduces to the upscaled variance of f_s for single shafts, as in Klammler et al. (2010a).

Fig. 1 shows an example of a quadruple square configuration (hereafter called Q) with respective shaft separation and variance-covariance matrices. The matrix in Fig. 1(c) is based on numerical integration of Eq. (6), where a spherical covariance function C_q is used with parameters $L/a_v = 5$ and $D/a_h = 0.1$. Based on the same principle of Eq. (6), the average of all the elements in the variance-covariance matrix of all shafts directly results in the respective variance reduction factor α_{sf} defined in Eq. (5). The shape of C'_s from Eq. (6) is not easily described analytically; however, its horizontal correlation range is known to be equal to $a_h + D$, corresponding to the minimum horizontal separation distance between shaft centers, for which all location pairs between shafts are beyond a_h and, thus, uncorrelated. Based on this, an approximation to C'_s, in the form of a spherical covariance function of range $a_h + D$, is proposed in Eq. (7), which avoids the numerical integration of Eq. (6) and allows for a quick and direct population of the respective shaft variance-covariance matrix, as shown in Fig. 1(d)

$$C'_q(h_s) \approx \begin{cases} 1 - 1.5\left(\frac{h_s}{a_h + D}\right) + 0.5\left(\frac{h_s}{a_h + D}\right)^3 & \text{for } \frac{h_s}{a_h + D} < 1 \\ 0 & \text{for } \frac{h_s}{a_h + D} \geq 1 \end{cases} \tag{7}$$

In addition to the quadruple configuration of Fig. 1(a), Fig. 2 illustrates further multiple shaft configurations considered in this work (D1, T1, and T2). In analogy to Fig. 1, for every configuration considered here and associated shaft separation distances, the variance-covariance matrices may be constructed using Eqs. (6) or (7), and α_{sf} may be found by averaging all matrix elements. The averaging of the matrix elements may be summarized by the following equations, where the type of foundation is indicated in the subscripts. Extensions to other group configurations not considered herein are straight-forward

$$\begin{aligned} \alpha_{sf,D1} &= 0.5C'_s(0) + 0.5C'_s(D_s) \\ \alpha_{sf,T1} &= 0.33C'_s(0) + 0.44C'_s(D_s) + 0.22C'_s(2D_s) \\ \alpha_{sf,T2} &= 0.33C'_s(0) + 0.67C'_s(D_s) \\ \alpha_{sf,Q} &= 0.25C'_s(0) + 0.5C'_s(D_s) + 0.25C'_s\left(\sqrt{2}D_s\right) \end{aligned} \tag{8}$$

For the exact solution of Eq. (6), values of C'_s and α_{sf} in Eq. (8) are a function of L/a_v, D/a_h, and D_s/D. For a typical value of $D_s/D = 3$ and using Eqs. (5) and (8), Fig. 3 graphically represents the outcome of the exact solution of $\alpha_{qf}^{1/2}$ for different shaft configurations (single shafts S from Klammler et al. 2010b is included for reference). Using the approximation of Eq. (7) (not shown for clearness of charts) instead of Eq. (6) results in maximum errors in $\alpha_{qf}^{1/2}$ (and hence CV_R for a given CV_q) of approximately ±5%. Errors are close to zero for $D/a_h < 0.05$, $D/a_h \approx 0.15$, and $D/a_h > 0.5$. For $0.05 < D/a_h < 0.15$ errors are negative (i.e., unconservative, which may be avoided by multiplication of $\alpha_{qf}^{1/2}$ by 1.05 in this range), while for $0.15 < D/a_h < 0.5$ errors are positive. Maximum positive and negative errors of the approximation also decrease as D_s/D increases and unconservative errors do not exceed 5% down to a theoretical value of $D_s/D = 1$ (results not shown).

The top graphs (case of $D/a_h = 0$) in Fig. 3 are all identical; in this case the variance reduction is independent of the number and arrangement of shafts and equal to variance reduction α_0 for averaging over a vertical line of length L (termed line shaft approximation in Klammler et al. 2010a, b). For a spherical covariance function

$$\begin{aligned} \alpha_0 &= 1 - \frac{L}{2a_v} + \frac{L^3}{20a_v^3} & &\text{for } 0 \leq \frac{L}{a_v} \leq 1 \\ \alpha_0 &= \frac{3a_v}{4L} - \frac{a_v^2}{5L^2} & &\text{for } \frac{L}{a_v} \geq 1 \end{aligned} \tag{9}$$

This is seen to be the common worst case scenario (maximum α_{qf} and CV_R) for all configurations in case of potentially unknown a_h. For $D/a_h > 0.5$, correlation between individual shafts is zero, and

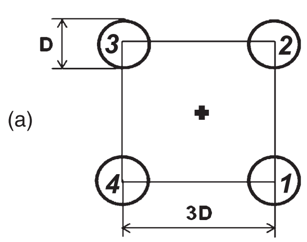

(b)	1	2	3	4
1	0	3	4.2	3
2	3	0	3	4.2
3	4.2	3	0	3
4	3	4.2	3	0

(c)	1	2	3	4
1	1	0.68	0.48	0.68
2	0.68	1	0.68	0.48
3	0.48	0.68	1	0.68
4	0.68	0.48	0.68	1

(d)	1	2	3	4
1	1	0.60	0.45	0.60
2	0.60	1	0.60	0.45
3	0.45	0.60	1	0.60
4	0.60	0.45	0.60	1

Fig. 1. (a) Example of quadruple Q square configuration with (b) shaft separation matrix in multiples of D; (c) and (d) are variance-covariance matrices in multiples of the upscaled single shaft variance σ_s^2

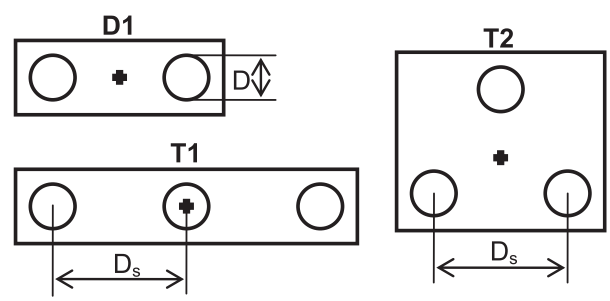

Fig. 2. Further examples of multiple shaft configurations with rigid pile caps and possible center borings (crosses)

J. Geotech. Geoenviron. Eng. 2013.139:84-94.

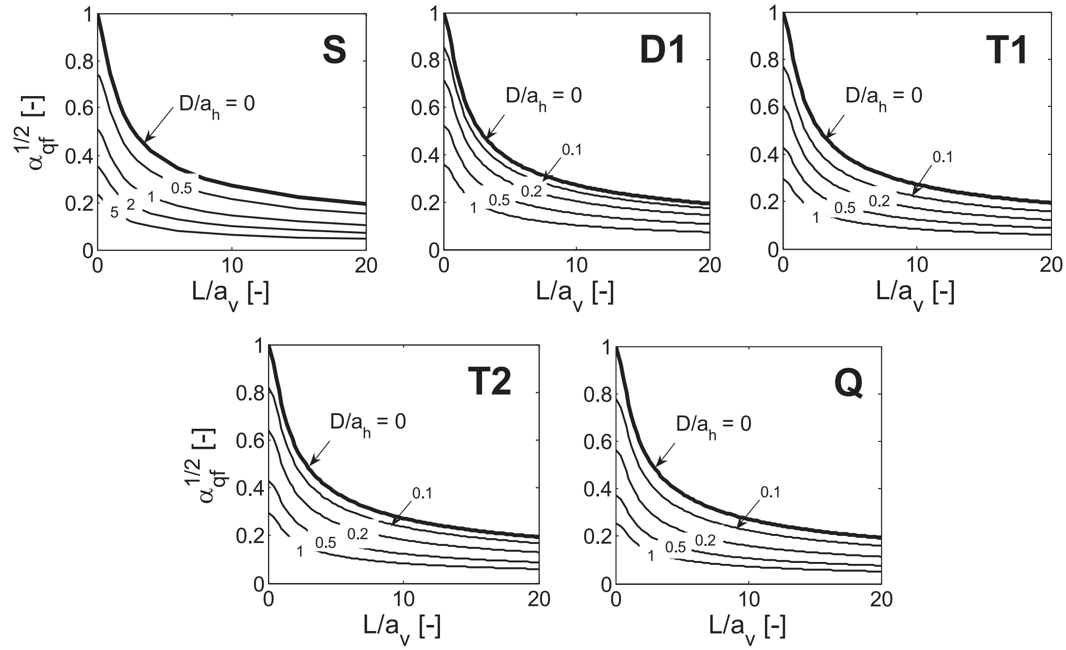

Fig. 3. Uncertainty reduction factor $\alpha_{qf}^{1/2}$ as a function of normalized shaft length L/a_v for single and multiple shaft configurations of Figs. 1 and 2 with normalized fundamental shaft separation distance $D_s/D = 3$; thick solid line corresponds to line shaft approximation $\alpha_0^{1/2}$

α_{sf} from shaft to foundation level becomes equal to $1/n_s$. Based on a computed CV_R and the assumption of lognormality for foundation resistance, determination of LRFD resistance factor Φ may be achieved along the lines of Klammler et al. (2010a) by the following AASHTO (2004) formulae:

$$\Phi = \frac{\lambda_R\left(\gamma_D\frac{Q_D}{Q_L} + \gamma_L\right)\sqrt{\frac{1 + \mathrm{CV}_Q^2}{1 + \mathrm{CV}_R^2}}}{\left(\lambda_{QD}\frac{Q_D}{Q_L} + \lambda_{QL}\right)\exp\left\{\beta\sqrt{\ln\left[\left(1 + \mathrm{CV}_R^2\right)\left(1 + \mathrm{CV}_Q^2\right)\right]}\right\}} \tag{10}$$

$$\mathrm{CV}_Q^2 = \frac{\left(\frac{Q_D}{Q_L}\lambda_{QD}\mathrm{CV}_{QD}\right)^2 + \left(\lambda_{QL}\mathrm{CV}_{QL}\right)^2}{\left(\frac{Q_D}{Q_L}\lambda_{QD}\right)^2 + 2\frac{Q_D}{Q_L}\lambda_{QD}\lambda_{QL} + \lambda_{QL}^2} \tag{11}$$

where CV_Q = coefficient of variation of the random load, β = user-selected reliability index depending on the importance of a structure (admissible probability of failure), and λ_R = prediction method specific resistance bias factor. The remaining dimensionless parameters in Eqs. (10) and (11) may be chosen according to AASHTO (2004) for load Cases I, II, and IV, where dead-load factor $\gamma_D = 1.25$, live-load factor $\gamma_L = 1.75$, dead-to-live load ratio $Q_D/Q_L = 2$, dead-load bias factor $\lambda_{QD} = 1.08$, live-load bias factor $\lambda_{QL} = 1.15$, dead-load coefficient of variation $\mathrm{CV}_{QD} = 0.128$, and live-load coefficient of variation $\mathrm{CV}_{QL} = 0.18$. Φ from Eq. (10) is based on CV_R of the whole foundation and, as such, assures a target probability of failure of the whole foundation and not just of a single shaft of the group (which would not be the actual design goal). The assumption of lognormality of R inherent in Eq. (10) appears to be plausible for two reasons: (1) q is a nonnegative quantity with typically pronounced positive skewness, such that a lognormal fit to q is likely to be appropriate, and (2) sums or integrals of lognormal variables, such as that of Eq. (2), are again well approximated by other lognormal distributions (Isaaks and Srivastava 1989). The latter is not contradictory to the central limit theorem, because lognormal distributions with decreasing coefficients of variation (e.g., because of spatial averaging) approach the normal distribution (Klammler et al. 2011).

Single and Multiple Shaft Foundations with Nearby Data

In practice, the assumption of an exhaustively sampled site may not be appropriate and additional uncertainty because of limited sampling may become significant. In contrast, knowing the exact locations of each foundation in the design process allows for collection of additional boring data inside or near the footprint of a foundation (e.g., at the center as indicated by crosses in Figs. 1 and 2 and considered hereafter). This may decrease uncertainty in predicted foundation resistances. To incorporate the influences of limited data and collocated borings, spatial correlations between borings and between borings and the foundation are explored. The geostatistical tool used for this purpose is ordinary kriging (Isaaks and Srivastava 1989; Journel and Huijbregts 1978), which delivers a predicted mean unit side friction f_f^* with an error variance σ_{fk}^2 between f_f^* and its true counterpart f_f. The resulting problem may be studied in a two-dimensional (horizontal) plane, where each of the n_b borings on a site is represented by a point associated to a data value equal to the mean q_{bi} $(i = 1, 2, \ldots, n_b)$ of the local strength observations in that boring (assuming that all borings are of approximately the same length L). The foundation is represented by its horizontal cross section centered on one of the borings, as illustrated by Fig. 4. For a full ordinary kriging solution, the horizontal covariances among all the borings themselves and between all the borings and the foundation would be required to determine a specific kriging weight w_i $(\sum w_i = 1)$ for each boring. f_f, as given by Eq. (2), is then predicted in the well know form

J. Geotech. Geoenviron. Eng. 2013.139:84-94.

Fig. 4. Exemplary plan view of borehole (crosses) and foundation locations (e.g., quadruple shaft foundation for a bridge site); not to scale

$$f_f^* = \sum_{i=1}^{n_b} w_i q_{bi} \tag{12}$$

with a variance σ_{fk}^2 of the prediction error $f_f^* - f_f$ as

$$\sigma_{fk}^2 = \sigma_f^2 + \sum_{i=1}^{n_b} \sum_{j=1}^{n_b} w_i w_j C_b(x_i - x_j) - 2 \sum_{i=1}^{n_b} w_i C_{bf}(x_i - x_f) \tag{13}$$

where C_b = horizontal covariance function of q_b, that is, a vertically upscaled version of C_q according to Eq. (6) with $\sigma_s^2 = 1$ and A_{s1} and A_{s2} reduced to borings (vertical lines) at locations x_i and x_j. In turn, C_{bf} is the horizontal covariance function between q_b and f_f, which may also be obtained from Eq. (6) using $\sigma_s^2 = 1$ in combination with A_{s1} as a vertical line at x_i and A_{s2} as A_f centered at location x_f. It is hereby assumed that the borings are sampled at intervals smaller than a_v such that additional sampling in a boring would only deliver highly redundant (i.e., correlated) information. With this, each boring may be considered as continuously sampled over depth, and the actual numbers of samples per boring become irrelevant [i.e., do not appear in Eqs. (12) and (13)]. The three terms on the right-hand side of Eq. (13) are the variance σ_f^2 of f_f [Eq. (4)], the variance σ_{f*}^2 of f_f^*, and twice the covariance $C(f_f^*, f_f)$ between f_f^* and f_f, whose negative sign reflects the benefit of conditioning data on prediction uncertainty.

In typical design situations the n_b borings at a site may consist of n_1 largely spaced borings from the preliminary site investigation (i.e., previous to the definition of foundation locations) and n_2 subsequent borings at potential foundation locations. In such cases, it may be reasonable to assume that no correlation exists between the borings at a site [i.e., $C_b(x_i - x_j) = C_b(0)$ for $i = j$ and equal to zero otherwise], except for when a preliminary boring happens to be in the vicinity of a future foundation location where a collocated boring is also obtained. In the latter case, it is conservative to consider full correlation between such nearby pairs of borings and reduce them to one effective boring by averaging. Thus, a conservative effective number of uncorrelated borings is obtained as $n_{be} \leq n_b$ (e.g., in Fig. 4 $n_b = 8$ and $n_{be} = 6$). With the further assumption that only the collocated boring ($i = 1$) presents possible spatial correlation with f_f [i.e., $C_{bf}(x_i - x_f) = C_{bf}(x_1 - x_f)$ for $i = 1$ and zero otherwise], a very simple ordinary kriging system may be constructed for determination of the kriging weights w_i, as represented by Eq. (14). w_1 represents the weight for the collocated boring, $w_2 = (1 - w_1)/(n_{be} - 1)$, the equal weights for all other borings ($w_i = w_2$ for $i > 1$), and μ is a Lagrangian operator

$$\begin{bmatrix} C_b(0) & 0 & \cdots & 0 & 1 \\ 0 & C_b(0) & \ddots & \vdots & \vdots \\ \vdots & \ddots & \ddots & 0 & \vdots \\ 0 & \cdots & 0 & C_b(0) & 1 \\ 1 & \cdots & \cdots & 1 & 0 \end{bmatrix} \begin{bmatrix} w_1 \\ w_2 \\ \vdots \\ w_{be} \\ \mu \end{bmatrix} = \begin{bmatrix} C_{bf}(x_1 - x_f) \\ 0 \\ \vdots \\ 0 \\ 1 \end{bmatrix} \tag{14}$$

Solving for w_1 and w_2 gives

$$\begin{aligned} w_1 &= \frac{1 + (n_{be} - 1)r}{n_{be}} \\ w_2 &= \frac{1 - r}{n_{be}} \end{aligned} \tag{15}$$

where $r = C_{bf}(x_1 - x_f)/C_b(0)$ is a normalized covariance between q_{b1} (collocated boring) and f_f (foundation). With Eq. (15) and $q_{bm} = 1/n_{be} \sum q_{bi}$ denoting the mean of all $i = 1, 2, \ldots, n_{be}$ effective borehole data, Eq. (12) may be written as

$$f_f^* = r q_{b1} + (1 - r) q_{bm} \tag{16}$$

For $r = 0$, the collocated boring has no more predictive power than the other borings and $f_f^* = q_{bm}$, while for $r = 1$ the collocated boring is a perfect predictor such that $f_f^* = q_{b1}$. Further, obtaining $\mu = C_b(0)(r - 1)/n_{be}$ and using $\sigma_{fk}^2 = \sigma_f^2 - w_1 C_{bf}(x_1 - x_f) - \mu$ (Isaaks and Srivastava 1989) gives

$$\alpha_{qfk} = \frac{\sigma_{fk}^2}{\sigma_q^2} = \alpha_0 \left[\frac{(1 - r)^2}{n_{be}} - r^2 \right] + \alpha_{qf} \tag{17}$$

as a respective variance reduction factor, which accounts for limited data through n_{be} and data conditioning through r. Theoretically, perfect prediction with $r = 1$ is only possible if the foundation is reduced to a vertical line (identical to the collocated boring), such that $\alpha_{qf} = \alpha_0$ correctly leading to $\alpha_{qfk} = 0$. For the opposite case of $r = 0$ (no conditioning to nearby data or random/unknown foundation location) and the conservative line shaft approximation ($\alpha_{qf} = \alpha_0$), Eq. (17) reduces to a respective expression developed in Klammler et al. (2010b) for the presence of a limited number of test borings. Finally, Eq. (17) is seen to correctly reduce to $\alpha_{qfk} = \alpha_{qf}$ of the previous section for $r = 0$ and $n_{be} \gg 1$, that is, no data conditioning and exhaustive data set available.

Eqs. (16) and (17) are directly valid for any type of single or multiple shaft foundation, and required values of α_0 and α_{qf} may be readily obtained from Fig. 3 and Eq. (9). What remains to be determined is the correlation parameter r, which is obtained from Eq. (6) with A_1 being a vertical line of length L (collocated boring) and A_2 being the total lateral foundation surface A_f. As such, Eqs. (16) and (17) are generally valid for arbitrary boring locations inside or nearby the foundation footprint. For the particular (but quite typical) case of a boring at the center of the footprint (i.e., $x_1 = x_f$), results from numerical integration of Eq. (6) are graphically represented in Fig. 5 as a function of a_h/D for various shaft configurations. As to be expected, spatial correlation in the vertical direction only has a small influence on the horizontal correlation parameter r, with this influence becoming quite insignificant for $L/a_v > 1$. The latter is also the range encountered in practical applications for which Fig. 5 is valid ($L/a_v < 1$ would be reflected by a nonstationary variogram over the foundation depths and would be handled by subtraction of a deterministic trend function such that $L/a_v > 1$ is again the case for the random residuals). For given foundation types (S, D1, T1, T2, or Q), dimensions (D and L ; $D_s = 3D$), and site conditions (q_{b1}, q_{bm}, CV_q, a_v, and a_h), Fig. 5 with Eqs. (16) and (17) can be used to find a nominal resistance R_n equal to

$$R_n = A_f f_f^* \tag{18}$$

A respective coefficient of variation CV_R results as

J. Geotech. Geoenviron. Eng. 2013.139:84-94.

$$\mathrm{CV}_R = \frac{\sigma_{qfk}}{f_f^*} = \frac{\sqrt{\alpha_{qfk}}}{1 + r\left(\frac{q_{b1}}{q_{bm}} - 1\right)}\mathrm{CV}_q \tag{19}$$

Assuming again that R is approximately lognormal, Eq. (10) may be used to find Φ.

Worst Case Scenario for Unknown a_h

As previously discussed, the horizontal correlation range a_h is a potentially unknown parameter because of a generally limited number of borings (i.e., horizontal information) at a site. One way of dealing with this problem is to adopt hypothetical values of a_h within a reasonable practical range and conservatively choose to design according to the worst case scenario, that is, where the resulting design load, or the product $R_n\Phi$, are a minimum. The equations for (numerically) minimizing $R_n\Phi$ are previously given; however, results will depend on a large number of case-specific parameters, such as foundation type, n_{be}, q_{b1}/q_{bm}, CV_q, β, and many more in Eqs. (10) and (11).

Pursued here is a simpler and more general method to conservatively minimize $R_n\Phi$ by minimizing each factor R_n and Φ separately. From Eq. (16), it is immediately seen that R_n is minimized to R_{nw} by equating f_f^* to the lower value between q_{b1} and q_{bm}

$$R_{nw} = A_f \min(q_{b1}, q_{bm}) \tag{20}$$

On the other hand, knowing that Φ for any value of β is a monotonically decreasing function in CV_R, Φ is minimized by maximizing CV_R to CV_{Rw} as

$$\mathrm{CV}_{Rw} = \frac{\sqrt{\alpha_{qfkw}}}{R_{nw}}\mathrm{CV}_q A_f q_{bm} \tag{21}$$

where α_{qfkw} is obtained by maximizing Eq. (17) as a function of a_h. This is best done numerically for different parameter combinations of foundation type, n_{be} and L/a_v. Knowing from Fig. 3 that α_{qf} in Eq. (17) may be well approximated by $k\alpha_0$, where k is primarily a function of a_h/D and, hence, r (not so much of L/a_v), an equation of the form

$$\alpha_{qfkw} \approx \left(A + \frac{B}{n_{be}}\right)\alpha_0 \tag{22}$$

is sought to approximate α_{qfkw}. For $D_s = 3D$ and with maximum errors in CV_{Rw} of approximately 1% on the unconservative and 5% on the conservative side, respective values of the coefficients A and B for each foundation type indicated in the index are obtained by trial and error fitting to exact numerical results as: $A_s = 0.17$, $B_s = 0.98$; $A_{D1} = 0.30$, $B_{D1} = 0.90$; $A_{T1} = 0.10$, $B_{T1} = 0.90$; $A_{T2} = 0.21$, $B_{T2} = 0.95$; and $A_Q = 0.18$, $B_Q = 0.97$. Hereby it may be consistently observed that the worst case scenarios for each individual foundation type occur for maximum values of a_h where r is still zero or small (Fig. 5), that is, where spatial averaging on A_f is limited and correlation to data in the footprint is equal or close to zero. Results of $(A+B/n_{be})^{1/2}$ of different foundation types are graphically illustrated in Fig. 6 (solid line) together with a previous solution for no center boring from Klammler et al. (2010b) for comparison (dashed line). Finally, the worst case scenario of Eq. (22) is independent of D, which contributes to maintaining the design process as simple as possible.

Other Sources of Uncertainty

In the previously mentioned equations, q is assumed to be an error-free measurement of the local unit side friction. Clearly, this is an assumption of ideal conditions, and an investigation of the effect of random (uncorrelated) measurement errors of variance σ_ε^2 at the sample scale is warranted. The latter should manifest as a nugget component (zero correlation range) in the variogram of q and may be accounted for by substituting $C_b(0)$ in Eq. (14) by $C_b(0) + \sigma_{\varepsilon b}^2$ (Kitanidis 1997). $\sigma_{\varepsilon b}^2$ is hereby the measurement error variance after vertical upscaling to the boring scale, and it is equal to σ_ε^2/n_s, with n_{samp} being an average number of samples per boring. Solving the modified system of equations, it is found that Eqs. (15)–(19) remain valid if modified parameters r_ε and $\alpha_{0\varepsilon}$, defined as

$$r_\varepsilon = \frac{r}{1 + e} \tag{23}$$

$$\alpha_{0\varepsilon} = \alpha_0(1 + e) \tag{24}$$

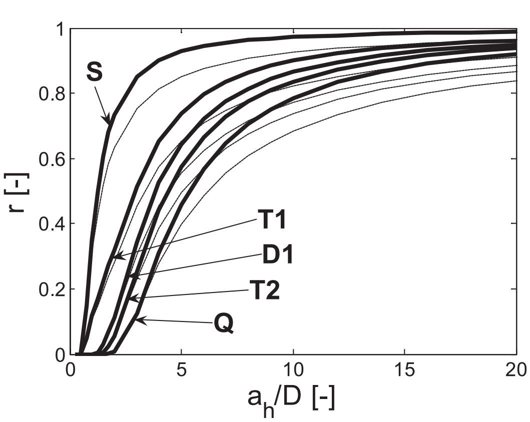

Fig. 5. Normalized covariance $r = C_{bf}(0)/C_b(0)$ between center boring and foundation as a function of normalized horizontal correlation range a_h/D for normalized shaft length $L/a_v > 1$ (continuous), $L/a_v = 0$ (dotted), and different shaft configurations ($D_s = 3D$)

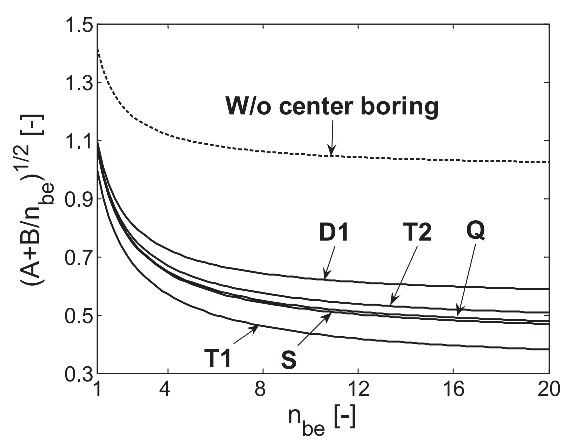

Fig. 6. Performance $(\alpha_{qfkw}/\alpha_0)^{1/2} = (A + B/n_{be})^{1/2}$ of different shaft configurations from Eq. (22) as a function of the effective number of borings n_{be}, assuming worst case scenario for unknown a_h with $\mathrm{CV}_\varepsilon = 0$ and presence of a center boring; dashed line for comparison from Klammler et al. (2010b) without a center boring

J. Geotech. Geoenviron. Eng. 2013.139:84-94.

are used instead of r and α_0. Parameter e results as the ratio between the variance components of measurement error and spatial variability at the boring scale

$$e = \frac{\sigma^2_{\varepsilon b}}{C_b(0)} = \frac{\sigma^2_\varepsilon}{n_{samp}\alpha_0\sigma^2_q} = \frac{\mathrm{CV}^2_\varepsilon}{n_{samp}\alpha_0\mathrm{CV}^2_q} \tag{25}$$

with $\mathrm{CV}_\varepsilon = \sigma_\varepsilon/q_{bm}$. Eqs. (20) and (21) remain valid as a worst case scenario if $\alpha_{0\varepsilon}$ is used instead of α_0 in Eq. (22). Approximation constants A and B are optimized for $\sigma^2_\varepsilon = 0$ and remain accurate for $e \leq 0.3$ with $n_{be} \geq 3$. Also, CV_q in Eqs. (19) and (21) has to be used as the coefficient of variation of spatial variability only (i.e., without measurement error). This means that if the coefficient of variation of collected q samples (including measurement error) is $\mathrm{CV}_{q\varepsilon}$, then $\mathrm{CV}_q = (\mathrm{CV}^2_{q\varepsilon} - \mathrm{CV}^2_\varepsilon)^{1/2}$. Furthermore, $\sigma^2_\varepsilon > 0$ does not affect the previously mentioned outcomes, where it is assumed that r is zero and n_{be} is very large, such that $\alpha_{qfk} = \alpha_{qf}$ in Eq. (17) (i.e., independent of r and α_0). Finally, CV_R from Eqs. (19) and (21) accounting for measurement error and spatial variability may be extended to a total foundation resistance uncertainty $\mathrm{CV}_{Rtot} = (\mathrm{CV}^2_R + \mathrm{CV}^2_{\mathrm{work}})^{1/2}$, where $\mathrm{CV}_{\mathrm{work}}$ is an independent compound workmanship uncertainty (e.g., randomness in shaft geometries, slurry handling), which is assumed to manifest at the foundation scale (as opposed to $\mathrm{CV}^2_\varepsilon$ at the sample scale).

Discussion of Results

The results developed are valid for both single and multiple shaft foundations with unknown or known foundation locations. In the latter case, nearby data may be considered to decrease resistance prediction uncertainty through spatial correlation (conditioning), where particular results given are for borehole data at the center of a foundation's footprint. Eqs. (16) and (17) are general in the sense that they encompass all of these scenarios and correctly collapse to the solution of Eqs. (6) and (8) for $n_{be} \gg 1$ and no data conditioning. However, explicit results for this particular scenario, as summarized in Fig. 3, are still valuable as input for the more general formulation, because it provides the parameter α_{qf} for Eq. (17).

Unknown Location of Foundation or no Nearby Data for Conditioning

In Fig. 3, the expected general tendency may be confirmed that the variance reduction monotonically increases as both L/a_v and D/a_h grow, that is, as the degree of spatial averaging increases. In the same way, increasing the number n_s of shafts in a foundation lowers resistance uncertainty. However, a direct comparison between different shaft configurations is not straightforward, because equal values of L and D lead to different values of A_f and, hence, nominal resistances for each case. In other words, different types of foundations are typically designed with different shaft dimensions. An exception to this is the triple shaft configurations T1 (row) and T2 (triangle), which perform identical for $D/a_h \geq 0.5$ (no correlation between individual shafts), and where T1 slightly outperforms T2 for $0 < D/a_h < 0.5$ because of the larger horizontal spreading of shafts in T1. Under the common practical situation of unknown horizontal correlation range a_h, Fig. 3 indicates that a respective worst case scenario exists by adopting $D/a_h = 0$, which reduces all foundation types to the same line shaft approximation of Klammler et al. (2010a, b). Finally, independent of the foundation type, shaft diameter, and correlation ranges, a general conclusion may be drawn from Fig. 3 that vertical averaging may be very efficiently explored up to $L/a_v \approx 4$ (steep portions of curves), while for $L/a_v > 4$ the benefits of increasing shaft length on uncertainty reduction (in absolute terms) become small.

Borehole Data at the Center of a Foundation Footprint

As reflected by Eqs. (17) or (22), this general conclusion about the efficiency of vertical averaging remains valid in the presence of a center boring in the footprint of a single or multiple shaft foundation. Moreover, a center boring has the benefit of leading to considerably more favorable worst case scenarios for unknown a_h. This is reflected by Fig. 6, where continuous graphs correspond to results from Eq. (22) and the dashed line represents $(1+1/n_{be})^{1/2}$, as derived in Klammler et al. (2010b) for an unknown foundation location (i.e., no center boring). This remains true even if no actual data conditioning between the center boring and the foundation exists (i.e., $r = 0$, such as considered for unknown foundation location), which is because of the mere fact that data were collected inside the foundation footprint and used in Eq. (16). Fig. 6 demonstrates that for a given number of borings n_{be}, the benefit of a center borings is a 50% reduction in CV_R. Provided a center boring is available, Fig. 6 also illustrates the performance of different shaft configurations in terms of resistance uncertainty. As previously mentioned, for each configuration, but assuming equal L/a_v [i.e., constant α_0 in Eq. (22)], some observations may be made. Independent of n_{be}, the configuration T1 (triple row) performs clearly best among all foundation types considered. T1 is followed by S (single), Q (quadruple), and T2 (triple triangle), which show similar behaviors, and finally D1 (double). The perhaps unexpectedly good performance of T1 may be attributed to the fact that the center boring falls exactly into the footprint of the center shaft, which reduces uncertainty substantially. In other words, data conditioning starts at lower a_h (compare Fig. 5) when horizontal averaging is still more effective as well. Eqs. (23) and (24) indicate that random measurement errors in q samples cause an effective reduction of correlation between the center boring and foundation, as well as an effective decrease in variance reduction over the borings. In combination with an uncertainty component at the foundation scale because of workmanship, this leads to increased values of α_{qfk} and α_{qfkw}.

Statistical Stationarity and Number of Borings

In all previously mentioned material, it is assumed that a site is statistically homogeneous, that is, the random function q is stationary (constant mean and variance). This implies that variogram sill and correlation ranges are defined, which is a necessary requirement for application of the Multiple Shaft Foundations without Nearby Data section. Hence, smooth spatial trends and discontinuities in statistical properties of q in the vertical or horizontal direction have to be removed prior to geostatistical treatment. In the same way as discussed in Klammler et al. (2010a) for single shafts, this may be achieved through detrending and subdivision of a site into homogeneous subzones (e.g., vertically into layers or horizontally into areas). In this respect, it is interesting to observe from Fig. 6 that prediction uncertainty may be efficiently reduced up to $n_{be} \approx 4$ (steep portions of graphs), while for $n_{be} > 4$ the benefit of additional borings on uncertainty reduction decreases. This fact is favorable for sites, which require horizontal division into subzones for separate geostatistical treatment, such that the n_{be}, for each subzone, becomes smaller. Moreover, in the presence of smooth horizontal trends over a site, n_{be} may be limited, without significantly inflating uncertainty, to a small number of nearest borings, which are used for design of a foundation (moving window

J. Geotech. Geoenviron. Eng. 2013.139:84-94.

approach; Journel and Rossi 1989). This may avoid introducing and making crucial decisions about the presence and shape of deterministic horizontal trend functions.

Example Problem

To demonstrate the application of the results presented, the case study of Klammler et al. (2010a) is extended by considering a triangle (T2) foundation with $L = 9$ m, $D = 0.4$ m, and the presence or not of a center boring for a reliability of $\beta = 3$. A total of 136 local rock strength (cohesion) measurements from six borings is available, where $q_{bm} = 2.28$ MPa with $CV_q = 0.50$. These data are obtained using $q = (q_u q_t)^{1/2}/2$, and, although further validation is recommended, a preliminary resistance bias factor $\lambda_R = 1.06$ is adopted for this prediction method [based on a comparison with load test data in FDOT (2003)]. A spherical covariance function is adopted with correlation ranges $a_v = 1.5$ m and $a_h = 4.5$ m for 80% of σ_q^2, plus $a_v = \infty$ and $a_h = 4.5$ m for the remaining 20% (i.e., 20% of the variability in q is only contained in the horizontal direction—random areal trend). For the purpose of illustrating the present approach, the six borings are assumed spatially uncorrelated among each other such that $n_{eb} = 6$.

Unknown Location of Foundation or No Nearby Data for Conditioning

In a first design step with an unknown foundation location or before obtaining data from a center boring, $R_n = A_f q_{bm} = 77.31$ MN, where $A_f = 3 \times 0.4 \times \pi \times 9 = 33.91$ m^2. Assuming that a_h and, consequently, $D/a_h = 0.4/4.5 = 0.09$ are known, Fig. 3 immediately gives a variance reduction factor for the first variogram component with $L/a_v = 9/1.5 = 6$ of $\alpha_{qf1} = 0.31^2$ and for the second variogram component with $L/a_v = 9/\infty = 0$ of $\alpha_{qf2} = 0.84^2$. Applying a result of Klammler et al. (2010a), α_{qf1} and α_{qf2} may be combined to a total variance reduction factor by taking the weighted average $\alpha_{qf} = 0.8\alpha_{qf1} + 0.2\alpha_{qf2} = 0.22$, such that $CV_R = 0.22^{1/2} \times 0.5 = 0.23$ and $\Phi = 0.63$ from Eq. (10) ($\Phi R_n = 48.71$ MN). In case a_h is not reliably known, the same chart of Fig. 3 gives worst case values of $\alpha_{01} = 0.35^2$ and $\alpha_{02} = 1$ by using $D/a_h = 0$. By the same relationships previously listed, this leads to $\alpha_0 = 0.30$, $CV_R = 0.27$, and a reduced $\Phi = 0.56$ ($\Phi R_n = 43.29$ MN). These results are very similar to those obtained for a single shaft in Klammler et al. (2010a), which may be attributed to the reduced shaft diameter for the triple configuration to achieve equal R_n.

Borehole Data at the Center of a Foundation Footprint

In a more advanced stage of the design process, data from a center boring at a foundation location may be available. Assuming that $a_h/D = 11.25$ is known and that the mean local strength observed in the center boring is $q_{b1} = 1.70$ MPa, respective values of $r_1 = 0.87$ (continuous line for $L/a_v = 6 > 1$) and $r_2 = 0.77$ (dashed line for $L/a_v = 0$) are obtained from Fig. 5, which may be combined by the same process of variance weighted averaging to a total value of $r = 0.8r_1 + 0.2r_2 = 0.85$. Eqs. (16) and (18) then give $f_f^* = 0.85 \times 1.70 + 0.15 \times 2.28 = 1.79$ MPa and $R_n = 33.91 \times 1.79 = 60.70$ MN. Furthermore, Eq. (17) may be evaluated with all parameters known, as previously stated, as $\alpha_{qfk}^{1/2} = [0.30(0.15^2/6 - 0.85^2) + 0.22]^{1/2} = 0.07$. Eq. (19) then gives $CV_R = 0.07 \times 0.5/(1 - 0.25 \times 0.85) = 0.044$, which translates into $\Phi = 0.97$ by Eq. (10), such that $\Phi R_n = 58.88$ MN. This is significantly larger than the previously obtained 48.71 MN in the absence of a center boring and with known $a_h = 4.5$ m, even though R_n is 25% smaller. If it is further assumed that the sampled data of q contained a measurement error of $CV_\varepsilon = 0.25$ (reliable quantification of this prediction method specific value is left for future investigation), one obtains $CV_q = (0.5^2 - 0.25^2)^{1/2} = 0.43$, $n_{samp} = 136/6 \approx 23$, $e = 0.25^2/(23 \times 0.30 \times 0.43^2) = 0.05$, $\alpha_{0\varepsilon} = 0.30(1 + 0.05) = 0.32$, $r_\varepsilon = 0.85/(1 + 0.05) = 0.81$, $f_f^* = 0.81 \times 1.70 + 0.19 \times 2.28 = 1.81$ MPa, $R_n = 1.81 \times 33.91 = 61.38$ MN, $\alpha_{qfk}^{1/2} = [0.32(0.19^2/6 - 0.81^2) + 0.22]^{1/2} = 0.11$, $CV_R = 0.11 \times 0.43/(1 - 0.25 \times 0.81) = 0.059$, $\Phi = 0.95$, and $\Phi R_n = 58.31$MN. This is not very much smaller than 58.88 MN for $CV_\varepsilon = 0$, which is because of the fact that independent measurement errors possess a larger tendency to cancel each other out (more effective variance reduction) than the spatially correlated variability in q. Furthermore, R_n slightly increased because of less weighting of q_{b1} versus q_{bm} for finding f_f^*. Finally, if additional errors because of workmanship of an assumed $CV_{\mathrm{work}} = 0.1$ are considered (i.e., workmanship is likely to affect nominal foundation resistance by less than approximately 10%; reliable quantification of this value is again left for future investigation), then $CV_{Rtot} = (0.059^2 + 0.1^2)^{1/2} = 0.12$, $\Phi = 0.84$, and $\Phi R_n = 51.56$ MN.

Worst Case Scenarios in the Presence of a Center Boring

Here the scenario of a center boring is considered, where $CV_\varepsilon = CV_{\mathrm{work}} = 0$ is assumed for a better illustration of effects of spatial variability. With a_h unknown, Fig. 7 graphically represents results of the design variables (with $A_f q_{bm}$ normalized to unity) as a function of a_h/D. Four different values of q_{b1}/q_{bm} are used, reflecting the results previously listed for $q_{b1}/q_{bm} = 0.75$ and $a_h/D = 4.5/0.4 = 11.25$. Most interesting to notice are the minima in ΦR_n (thick continuous lines), which can be explored in design as worst case scenarios for unknown a_h. For q_{b1}/q_{bm} close to or larger than 1, these minima are mainly conditioned by minima in Φ (i.e., prediction uncertainty) and consistently occur near the point where correlation between center boring and foundation starts. In contrast, for q_{b1}/q_{bm} significantly smaller than 1, the minima may occur for very large values of a_h/D, thus being conditioned by small values of R_n without significant prediction uncertainty ($CV_R \approx 0$). In the previously considered case of $q_{b1}/q_{bm} = 0.75$, for example, a worst case value of $\Phi R_n = 0.73 A_f q_{bm} = 56.44$ MN is obtained being only slightly smaller than 58.88 MN for known $a_h = 4.5$ m. As evident from Fig. 7, the potential increase in ΦR_n because of a known a_h becomes larger as q_{b1}/q_{bm} grows. Considering only worst case scenarios, however, benefits in ΦR_n because of larger q_{b1}/q_{bm} (i.e., stronger ground at the foundation location) are not very significant in the present case. An improvement upon the minima in ΦR_n of Fig. 7 can be possible by explicitly taking into account the spatial correlation structures between all borings (i.e., improving on the conservative assumption that two nearby borings are fully correlated) and by allowing for correlation between more than a single boring with the foundation. However, this would quickly lead to an increased computational complexity, because an ordinary kriging system has to be solved for every value of a_h/D instead of the simplified Eqs. (16) and (17). Even evaluation of worst case scenarios, as in Fig. 7, based on Eqs. (16) and (17), may soon become a tedious task without computational aid, and even more conservative worst case scenarios are indicated inside the charts based on the approximate Eqs. (20)–(22). For the example problem with $q_{b1}/q_{bm} = 0.75$, this results in $R_{nw} = 0.75 A_f q_{bm} = 57.99$ MN, $\alpha_{qfkw} = (0.21 + 0.95/6) \times 0.30 = 0.11$, $CV_{Rw} = 0.11^{1/2} \times 0.5/0.75 = 0.22$, $\Phi_w = 0.65$, and $\Phi_w R_{nw} = 37.69$ MN, which presents a relatively large decrease in admissible load with respect to 56.44 MN, based on simultaneous minimization of the product ΦR_n rather than of each factor separately. However, as illustrated by Fig. 7, this

J. Geotech. Geoenviron. Eng. 2013.139:84-94.

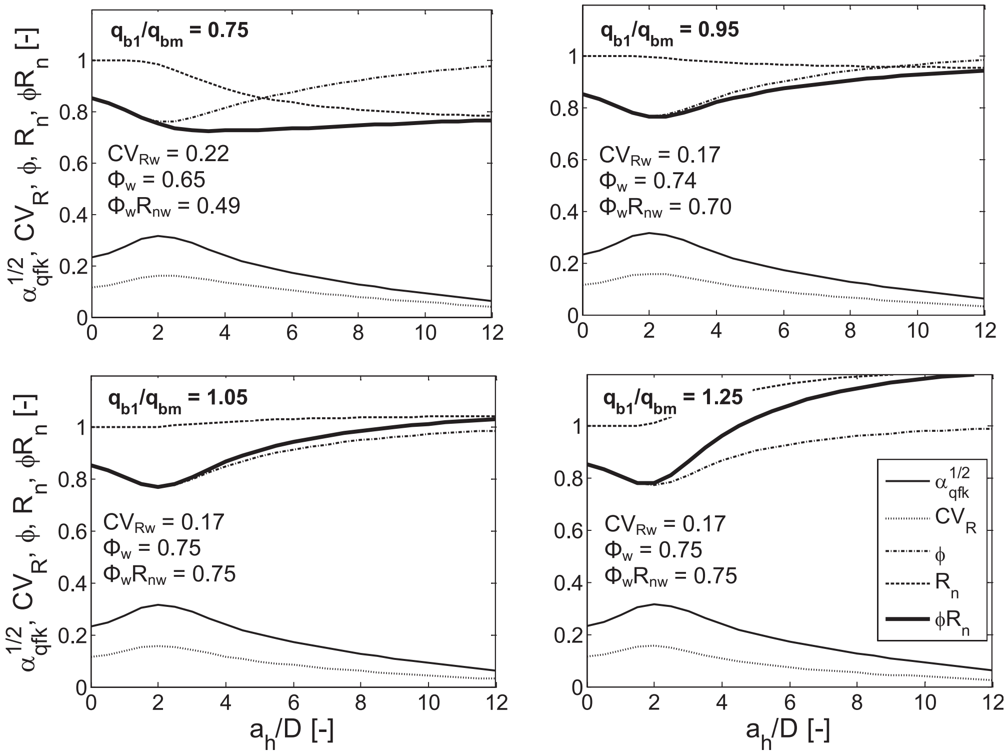

Fig. 7. Exact (graphs) and approximate (text) worst case scenarios for example problem with $CV_\varepsilon = 0$ and different values of q_{b1}/q_{bm}

conservative difference decreases quickly as q_{b1}/q_{bm} approaches or exceeds unity. This indicates that an additional mathematical effort to directly minimize the product ΦR_n may be quite compensating, especially for $q_{b1}/q_{bm} < 1$.

Summary

LRFD aims at rationally accounting for uncertainties in the design process to meet prescribed target probabilities of failure. For this purpose, the influence of spatially variable soil/rock strength (cohesion at zero confining pressure) on axial resistance and uncertainty due to side friction of single and multiple shaft foundations is analyzed. According to practice in Florida limestone (FDOT 2011), contributions of end-bearing resistance are neglected. Based on a geostatistical approach, resistance uncertainties are evaluated in a spatial upscaling and ordinary kriging framework. For the scenario of a center boring inside the footprint of a foundation, a general solution is presented, which accounts for the total amount of borings at a site (i.e., limited data), possible correlation between a center boring and the foundation, random measurement errors, as well as uncertainties because of workmanship. For the common situation of unknown horizontal correlation range, two conservative ways of assessing worst case scenarios are defined. One minimizes the product ΦR_n and requires a larger computational effort, the other minimizes Φ and R_n separately, which simplifies calculations, but may substantially increase conservativism. Worst case scenarios are seen to be independent of shaft diameter, and an example problem is presented to illustrate the process and some of its mechanisms. The approach aims at directly meeting prescribed probabilities of failure (reliabilities) of whole foundations rather than single objects of a foundation. An interesting observation is that the uncertainty reduction because of additional data becomes quite small for more than approximately four borings. This indicates that a so-called moving window approach may be appropriate, where only a few nearest borings to a foundation are considered for design. Crucial decisions about presence and shape of possible horizontal trends may, thus, be avoided. In analogy to Klammler et al. (2010a), results of the present work may also be directly extended to different spatial covariance functions than the spherical one (e.g., exponential) and to situations of nested variogram structures (see example problem) and vertical layering in ground properties.

Acknowledgments

This research was supported by the Florida Department of Transportation Contract No. BD-545, RPWO #76, entitled "Modification of LRFD Resistance Factors Based on Site Variability." The boring and laboratory test results for the example problem were obtained by the State Materials Office of the Florida Department of Transportation. The first author also acknowledges support by a fellowship of the Bahia State Science Foundation (FAPESB; DCR 0001/2009), Brazil.

Notations

The following symbols are used in this paper:

- A, B = constants for approximation of α_{qfkw};
- A_f = lateral surface area of all shafts in a foundation;
- A_s = lateral surface area of one shaft;
- a_h = horizontal correlation range;
- a_v = vertical correlation range;
- C_b = spatial covariance function of q_b (boring scale);
- C_{bf} = spatial covariance between the foundation and nearby boring;
- C_q = spatial covariance function of q (point scale);

C_s = spatial covariance function of f_s (shaft scale);
C'_q = normalized spatial covariance function of q (point scale);
C'_s = normalized spatial covariance function of f_s (shaft scale);
CV_Q = coefficient of variation of the design load;
CV_{QD} = coefficient of variation of the dead load;
CV_{QL} = coefficient of variation of the live load;
CV_q = coefficient of variation of q (only spatial variability without measurement error);
CV_R = coefficient of variation of foundation resistance;
CV_{Rtot} = coefficient of variation of foundation resistance including construction workmanship uncertainty;
CV_{Rw} = CV_R under worst case scenario for unknown a_h;
$\mathrm{CV}_{\mathrm{work}}$ = coefficient of variation of construction workmanship uncertainty (acting at the foundation scale);
CV_ε = coefficient of variation of measurement error in q;
$\mathrm{CV}_{q\varepsilon}$ = coefficient of variation of measured q (including spatial variability and measurement error);
D = shaft diameter;
D_s = fundamental shaft center separation distance (e.g., $3D$);
dA = infinitesimal areal element for integration over shaft surfaces;
e = ratio between variances of measurement error and spatial variability in q at the boring scale;
f_f = unit side friction at the foundation scale;
f_f^* = estimate of f_f;
f_s = unit side friction at the shaft scale;
h = spatial separation vector (lag distance);
h_h = horizontal lag distance;
h_{iso} = normalized isotropic lag distance;
h_s = lag distance between shaft centers;
h_v = vertical lag distance;
i = index variable;
L = shaft length;
n_b = number of borings at the site;
n_{be} = effective number of uncorrelated borings at the site;
n_s = number of shafts in the foundation;
n_{samp} = average number of samples per boring;
n_1 = number of borings from the preliminary site investigation;
n_2 = number of borings at the potential foundation locations;
Q_D/Q_L = dead-to-live load ratio;
q = measured unit side friction at the point scale (strength or cohesion at zero confining pressure);
$q_{b(i)}$ = mean unit side friction at the boring scale (in ith boring);
q_{bm} = mean unit side friction over all n_{be} borings;
q_t = split tension strength;
q_u = unconfined compression strength;
R = random foundation resistance;
R_n = nominal foundation resistance (mean of R);
R_{nw} = R_n under worst case scenario of unknown a_h;
r = normalized covariance between nearby boring and foundation;
r_ε = effective value of r when considering measurement error in q;
$w_{i,j}$ = ordinary kriging weights;
x = coordinate vector;
x_f = foundation location;
$x_{i,j}$ = boring locations;
α_{qf} = variance reduction factor between q (point scale) and f_f (foundation scale);
α_{qfk} = variance reduction factor between q (point scale) and the estimation error of f_f (foundation scale) in the presence of a nearby boring using kriging weights;
α_{qfkw} = variance reduction factor α_{qfk} under the worst case scenario for unknown a_h;
α_{qs} = variance reduction factor between q (point scale) and f_s (shaft scale);
α_{sf} = variance reduction factor between f_s (shaft scale) and f_f (foundation scale);
α_0 = variance reduction factor between q (point scale) and q_b (boring scale/vertical line);
$\alpha_{0\varepsilon}$ = effective value of α_0 when considering measurement error in q;
β = LRFD reliability index;
γ_D = dead-load factor;
γ_L = live-load factor;
λ_R = resistance bias factor;
λ_{QD} = dead-load bias factor;
λ_{QL} = live-load bias factor;
μ = Lagrangian operator;
μ_f = mean of f_f;
μ_s = mean of f_s;
μ_q = mean of q;
ρ = recovery;
σ_f^2 = variance of f_f (foundation scale);
σ_{fk}^2 = estimation error variance of f_f if there is a boring near the foundation and when using kriging weights;
σ_q^2 = variance of q (point scale);
σ_s^2 = variance of f_s (shaft scale);
σ_ε^2 = variance of measurement error in q (point scale);
$\sigma_{\varepsilon b}^2$ = variance of measurement error after upscaling to q_b (boring scale);
Φ = LRFD resistance factor; and
Φ_w = Φ under worst case scenario for unknown a_h.

References

AASHTO. (2004). *LRFD bridge design specifications*, 3rd Ed., AASHTO, Washington, DC.

Brustamante, M., and Gianeselli, L. (1982). "Pile bearing capacity prediction by means of static penetrometer, CPT." *Proc., 2nd Eur. Symp. Penetrometer Test.*, Vol. 2, A.A. Balkema Publishers, Leiden, Netherlands 493–500.

Chung, J., Ko, J., Klammler, H., McVay, M., and Lai, P. (2011). "A numerical and experimental study of bearing stiffness of drilled shafts socketed in heterogeneous rock." *Comput. Struct.*, 90–91, 145–152.

Fenton, G. A., and Griffiths, D. V. (2002). "Probabilistic foundation settlement on spatially random soil." *J. Geotech. Geoenviron. Eng.*, 128(5), 381–390.

Fenton, G. A., and Griffiths, D. V. (2003). "Bearing-capacity prediction of spatially random c—φ soils." *Can. Geotech. J.*, 40(1), 54–65.

Fenton, G. A., and Griffiths, D. V. (2005). "Three-dimensional probabilistic foundation settlement." *J. Geotech. Geoenviron. Eng.*, 131(2), 232–239.

J. Geotech. Geoenviron. Eng. 2013.139:84-94.

Fenton, G. A., Griffiths, D. V., and Cavers, W. (2005). "Resistance factors for settlement design." *Can. Geotech. J.*, 42(5), 1422–1436.
Fenton, G. A., Griffiths, D. V., and Zhang, X. Y. (2008). "Load and resistance factor design of shallow foundations against bearing failure." *Can. Geotech. J.*, 45(11), 1556–1571.
Florida Department of Transportation (FDOT). (2003). "Static and dynamic field testing of drilled shafts: Suggested guidelines on their use for FDOT structures." *Rep. No. 99052794*, FDOT, Gainesville, FL.
Florida Department of Transportation (FDOT). (2011). *Soils and foundations handbook*, FDOT, Gainesville, FL.
Foye, K. C., Salgado, R., and Scott, B. (2006). "Assessment of variable uncertainties for reliability-based design of foundations." *J. Geotech. Geoenviron. Eng.*, 132(9), 1197–1207.
Haldar, S., and Sivakumar Babu, G. L. (2008). "Load resistance factor design of axially loaded pile based on load test results." *J. Geotech. Geoenviron. Eng.*, 134(8), 1106–1117.
Isaaks, E. H., and Srivastava, R. M. (1989). *An introduction to applied geostatistics*, Oxford University Press, Oxford, U.K.
Journel, A. G., and Huijbregts, C. J. (1978). *Mining geostatistics*, Blackburn Press, Caldwell, NJ.
Journel, A. G., and Rossi, M. E. (1989). "Do we need a trend model in kriging?" *Math. Geol.*, 21(7), 715–739.
Kitanidis, P. K. (1997). *Introduction to geostatistics: Applications to hydrogeology*, Cambridge University Press, Cambridge, U.K.
Klammler, H., Hatfield, K., McVay, M., and Luz, J. (2011). "Approximate upscaling of geo-spatial variables applied to deep foundation design." *Georisk. Assess. Manage. Risk Eng. Syst. Geohazards*, 5(3–4), 163–172.
Klammler, H., McVay, M., Horhota, D., and Lai, P. (2010a). "Influence of spatially variable side friction on single drilled shaft resistance and LRFD resistance factors." *J. Geotech. Geoenviron. Eng.*, 136(8), 1114–1123.
Klammler, H., McVay, M., Lai, P., and Horhota, D. (2010b). "Incorporating geostatistical aspects in LRFD design for deep foundations." *ASCE Geotechnical Special Publication GeoFlorida 2010: Advances in Analysis, Modeling and Design* (CD-ROM), E. O. Fratta, B. Muhunthan, and A. J. Puppala, eds., Vol. 199, ASCE, Reston, VA.
Paice, G. M., Griffiths, D. V., and Fenton, G. A. (1996). "Finite element modeling of settlements on spatially random soil." *J. Geotech. Eng.*, 122(9), 777–779.
Phoon, K. K., and Kulhawy, F. H. (1999a). "Characterization of geotechnical variability." *Can. Geotech. J.*, 36(4), 612–624.
Phoon, K. K., and Kulhawy, F. H. (1999b). "Evaluation of geotechnical variability." *Can. Geotech. J.*, 36(4), 625–639.
Phoon, K. K., Kulhawy, F. H., and Grigoriu, M. D. (2003). "Development of a reliability-based design framework for transmission line structure foundations." *J. Geotech. Geoenviron. Eng.*, 129(9), 798–806.
Popescu, R., Deodatis, G., and Nobahar, A. (2005). "Effects of random heterogeneity of soil properties on bearing capacity." *Prob. Eng. Mech.*, 20(4), 324–341.
Sivakumar Babu, G. L., Srivastava, A., and Murthy, D. S. N. (2006). "Reliability analysis of the bearing capacity of a shallow foundation resting on cohesive soil." *Can. Geotech. J.*, 43(2), 217–223.
Zhang, L. M., Tang, W. H., and Ng, C. W. W. (2001). "Reliability of axially loaded driven pile groups." *J. Geotech. Geoenviron. Eng.*, 127(12), 1051–1060.
Zhang, L. M., Xu, Y., and Tang, W. H. (2008). "Calibration of models for pile settlement analysis using 64 load tests." *Can. Geotech. J.*, 45(1), 59–73.